THE STUDY OF ROCKFILL DAMS PROBLEMS: PHYSICAL MODELS AND TESTS ON GRANULAR MATERIALS

Pier Paolo ROSSI
ISMES, Bergamo

1. FOREWORD

ISMES, in collaboration with ENEL, has carried out wide-ranging research for the study of problems related to rockfill dams. This joint effort was directed into researching the two fields detailed below:

a) laboratory tests on prototype granular material to determine the principal mechanical characteristics. Our attention was focused in particular on the definition of two basic parameters: the compressibility characteristics and the angle of internal friction. With a view to ensuring fair reliability of the results, the tests were carried out on large specimens (diameter $\phi \geqslant 50$ cm)

b) study by physical models in reduced scale (1 : 120) of rockfill dams with different geometric characteristics for the study of the behaviour of the embankments from the point of view of settlements and stress distribution.
The models have been realized principally for basic research and do not refer to any real case.
A simplifying hypothesis has been assumed at the base of our research: we have considered only a single type of rockfill dam with waterproof coating on the upstream face in order to eliminate any kind of problem due to the presence of water pressure within the embankment. The problem of simulating pore-pressure effect would be too difficult to solve by means of physical models.

2. EXPERIMENTAL RESEARCH ON PROTOTYPE GRANULAR MATERIALS

2.1 Compressibility tests with confined lateral deformation

A special aedometric chamber (fig. 1) has been designed by ISMES for the determination of compressibility characteristics in condi-

FIG. 1

Aedometric chamber for compressibility tests on granular material.

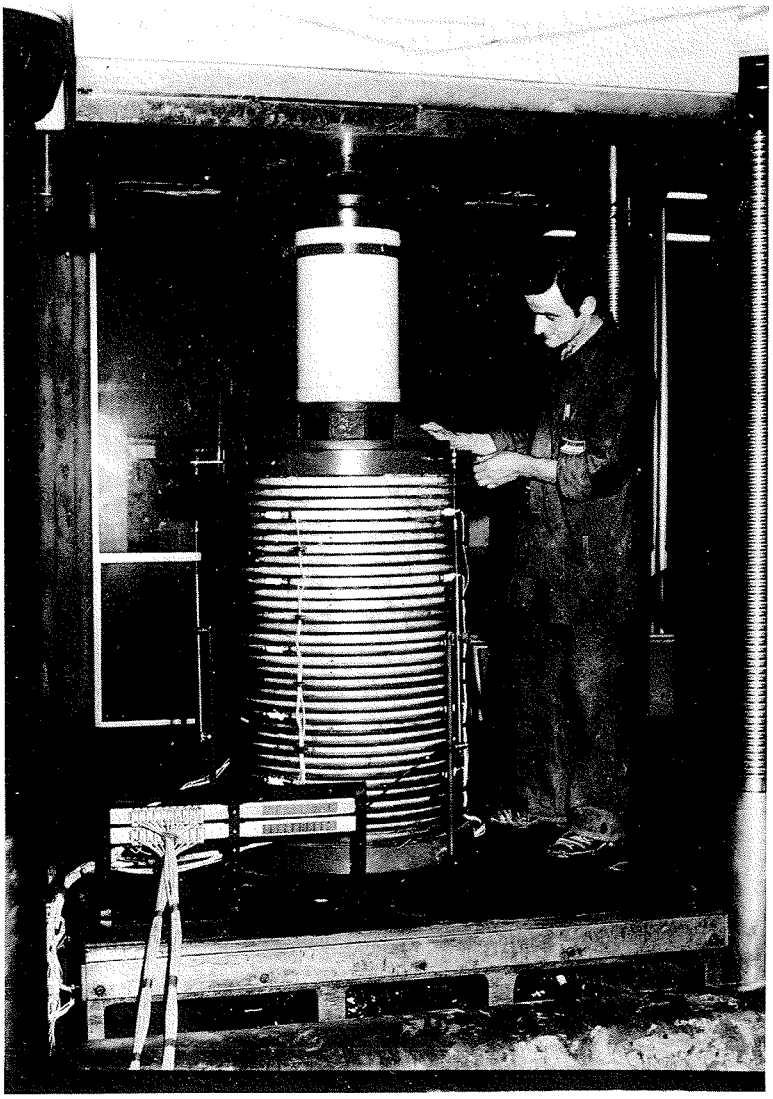

tion of confined lateral deformation. To minimize the friction effect between the granular material and the wall of the chamber, use was made of a series of alternating rigid and deformable rings glued to one another. While the rigid lateral confinement is provided, the presence of highly deformable rings, alternated with the rigid ones, makes it possible to obtain a very low contribution to resistance against the axial compressive load. The rigid rings are equipped with strain-gauges which allow the confining pressure to be measured during the test.

According to the maximum grain-size, the tests are carried out in chambers of different diameter up to 120 cm (the heigth of the chamber is equal to twice its diameter). It is advisable to adopt a value of the ratio between the maximum grain-size and the diameter of the chamber not higher than 0.2.

As is well-known, the compressibility of the granular material is influenced by several parameters.

As an example, fig. 2 illustrates the influence on the compressibility of a marly-limestone specimen of the initial percentage of

FIG. 2

Compressibility curves with different values of the initial percentage of voids (v_i%).

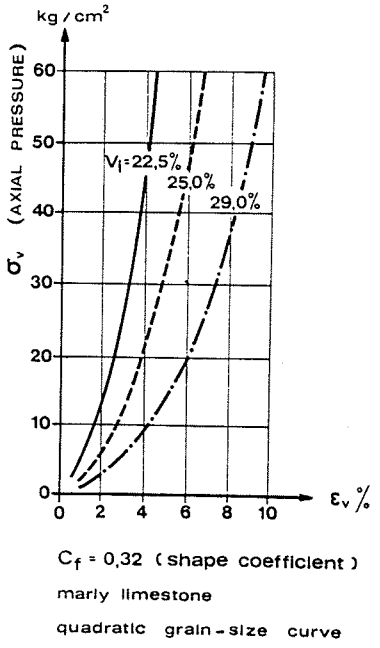

voids (v_i%), which is a parameter defining the initial consolidation of the specimen.

Another parameter which influences the compressibility of a granular material is the shape coefficient C_f defined as the ratio between the volume of a certain number of grains and the sum of the corresponding circumbscribing spheres:

$$C_f = \frac{\sum_o^n V}{\sum_o^n \frac{\pi}{6} D^3} \qquad n \geqslant 100$$

Fig. 3 shows the influence of the shape coefficient C_f on the compressibility of a marly-limestone specimen at constant value of V_i%. It can be seen that the compressibility increases with the increase of the shape coefficient.

The compressibility tests may be carried out on dry or saturated material with the possibility of saturating the specimen during the test at constant axial load. Fig. 4 shows a comparison between the results of tests on dry (curve 1) and saturated specimen (curve 2) of the same material. A third test (curve 3) was carried out on a initially dry specimen saturated at the constant load of 15 Kg/cm^2; it can be observed that after the saturation, for further increase of load, the material follows the curve 2 relative to the initially saturated specimen.

2.2 Triaxial tests

The second basic parameter which defines the mechanical characteristics of a granular material is the angle of internal friction.

For the evaluation of this parameter the special triaxial equip

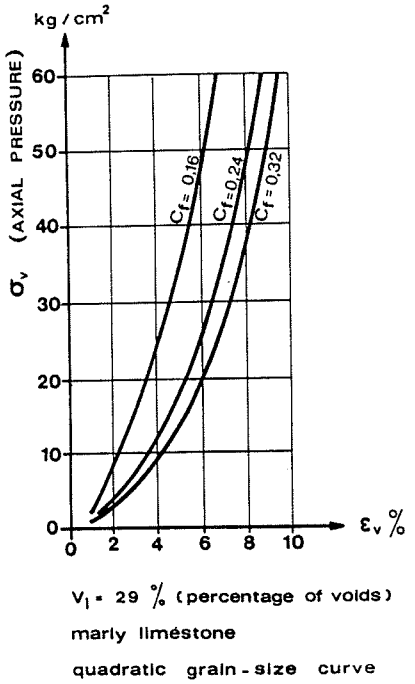

V_i = 29 % (percentage of voids)
marly limestone
quadratic grain-size curve

FIG. 3

Influence of the shape coefficient (C_f) on the compressibility.

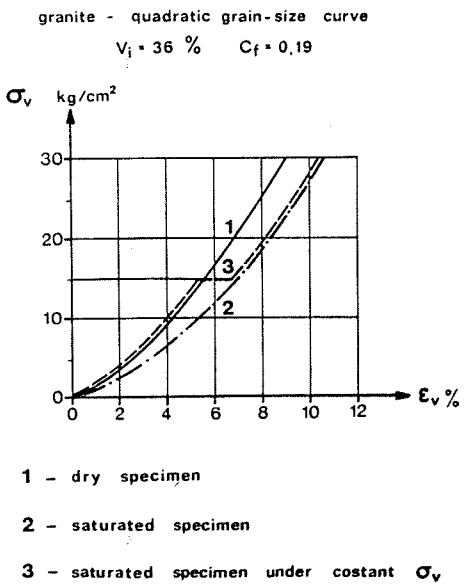

1 - dry specimen

2 - saturated specimen

3 - saturated specimen under costant σ_v

FIG. 4

Compressibility tests on dry and saturated specimens.

ment shown in fig. 5 was developed for tests on specimens of large dimensions (diameter 35 cm, height 70 cm). The specimen is covered by a PVC membrane able to prevent piercing by contact with the sharp-edged points of the rock material.

FIG. 5

Triaxial test cell for granular material.

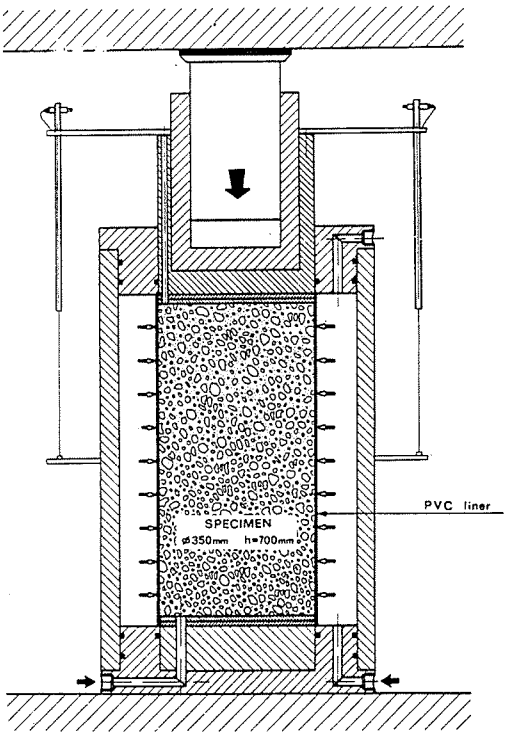

The utmost care has to be taken in the preparation of the specimen. On the basis of the desired grain-size curve, the specimen is cast by layers into a special molder and assessed by plate vibrator in order to obtain the desired initial percentage of voids $V_i\%$. Then the molder is removed and the wall of the chamber is mounted.

The axial deformations of the specimen are measured by means of inductive transducers and, through the measurement of the volume of liquid in the test chamber, it is possible to determine the volume changes and the average cross-section changes.

A typical result of the behaviour of a granular material under triaxial stress conditions is shown in fig. 6.

FIG. 6

Typical results of triaxial test for different values of confining pressure.

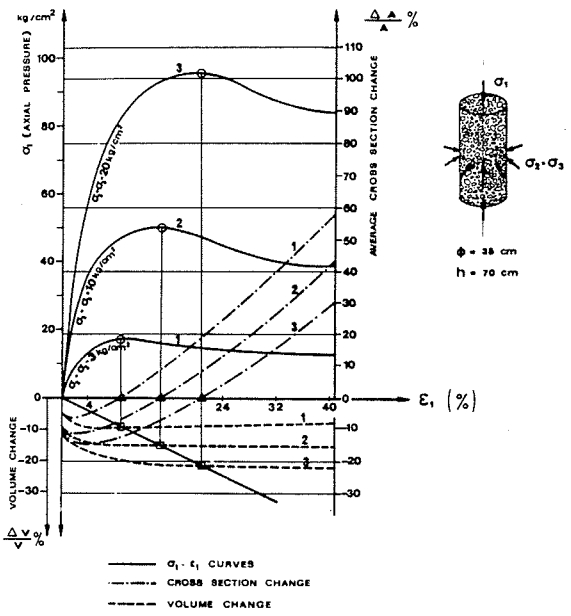

Three families of curves are represented:

- axial stress versus axial deformation curves at constant confining pressure (3-10-20 Kg/cm^2); these curves clearly show that a peak strength and a residual one can be identified;
- average cross-section change curves;
- volume change curves.

The initial volume decreases to a minimum corresponding to the peak strength, then it becomes constant. As regards average cross-section it can be observed that there is an initial decrease, then a rapid increase. It is interesting to notice that the peak strength occurs when the average cross-section practically reverts to its initial values.

3. PHYSICAL MODELS OF ROCKFILL DAMS

On the basis of the parameters determined by the above-mentioned tests, a wide experimental investigation was carried out on several models constructed of granular material reproducing in similitude the mechanical properties of the prototype material.

The following similitude parameters were adopted:

$$\lambda = L_P / L_M$$

$$\zeta = E_P / E_M$$

$$\rho = \gamma_P / \gamma_M$$

P = prototype

M = model

$$\lambda = \zeta = 120$$

$$\rho = 1$$

At first a section of a continuous embankment was reproduced. Then three models were made, with the same ratio between the height and the width and with different values of the angles of inclination of lateral abutments (30^o, 50^o, 70^o) (fig. 7).

FIG. 7

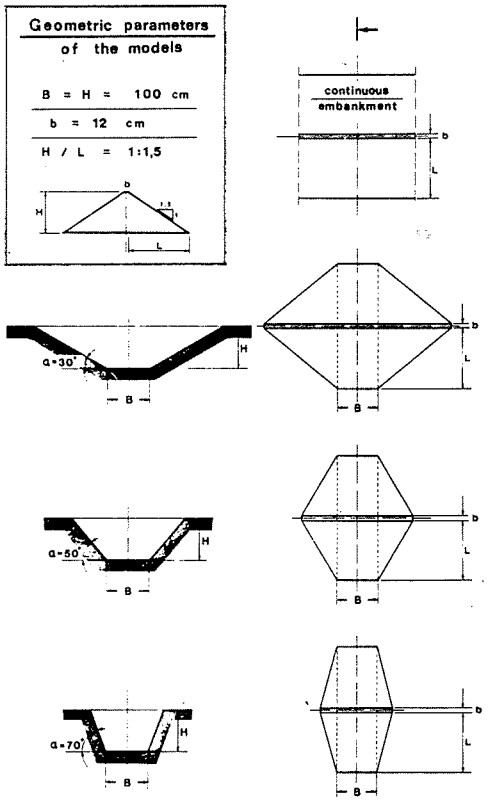

Two additional models were set up, having a "V" shaped valley and two different angles of inclination of lateral abutments (30^{o}, 50^{o}) (fig. 8). In all the models the embankment slope, symmetrical for both faces, was 1 : 1.5.

FIG. 8

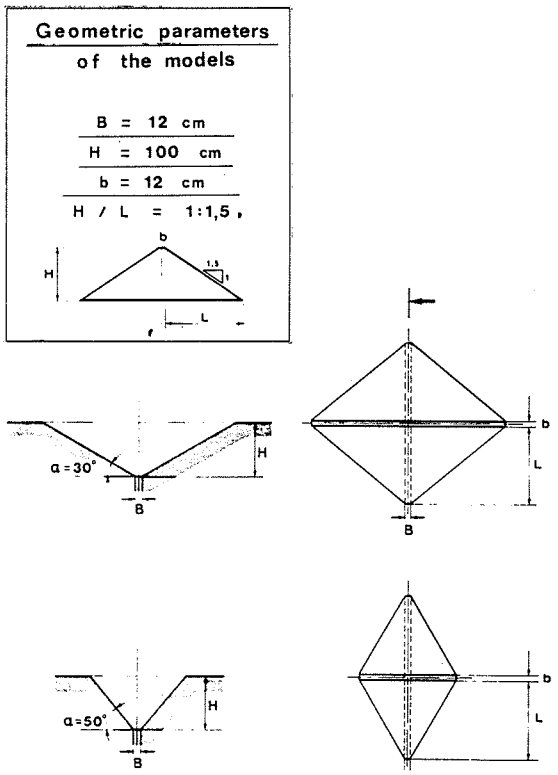

3.1 Model material

The composition of the model material is as follows:

Pumice	(powder)	12 %
Baryte	(powder)	81 %
Water		5 %
Glicerine		1,5 %
Epoxy resin		0,5 %

The material is moulded in brickets, than cured in steam and crushed to reproduce the desired granulometric curve.

The physical-mechanical characteristics of the brickets are as follows:

Specific gravity	$\gamma = 2,4 \quad t / m^3$
Deformability modulus at 10% σ_c	$E_d = 5000 \div 6000 \quad kg / cm^2$
Uniaxial compression strength	$\sigma_c = 10 \div 12 \quad kg / cm^2$

Compressibility tests have been carried out on the granular material using a special aedometer with alternating rigid and deformable rings of the same type as that used for the prototype material (fig. 1).

The compressibility curve shown in fig. 9 reproduces in the desired scale the deformability behaviour of the prototype material and represents the main parameter taken into account in the study of the model.

FIG. 9

Compressibility curve of the granular model material.

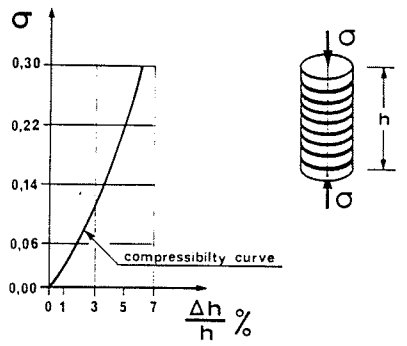

γ_a = 1,9 t / m³

maximum grain size = 10 mm

shape coefficient : C_f = 0,35÷0,40

3.2 Modelling technique

The models rest on a rigid foundation and the construction of the embankments is realized by the layout of 5 cm thick layers. A special vibrator was employed to achieve the desired initial percentage of voids.

Hydrostatic load was applied to the upstream face by means of liquid contained in a rubber bag.

Stress-meter cells were installed on the rigid foundation to measure the stress distribution on the base of the embankments.

Both vertical and horizontal settlements were measured along four different levels inside the embankment by means of special devices, designed by ISMES, with wires kept in tension by springs.

Displacement transducers were also installed on the surface of the embankment.

Fig. 10 shows a view of a model during the construction, while fig. 11 provides a view of a model during hydrostatic load tests.

FIG. 10

View of a model (with a "V" shaped valley) during the construction. Vertical and horizontal settlement measuring devices are visible.

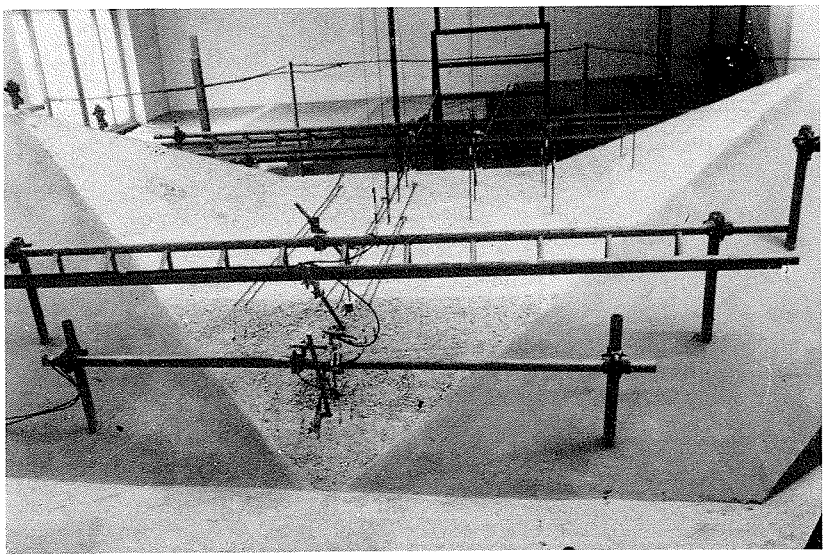

FIG. 11

View of a model during the tests. Visible on the upstream face is the hydrostatic load equipment and on the downstream face the instrumentation for settlement measurements.

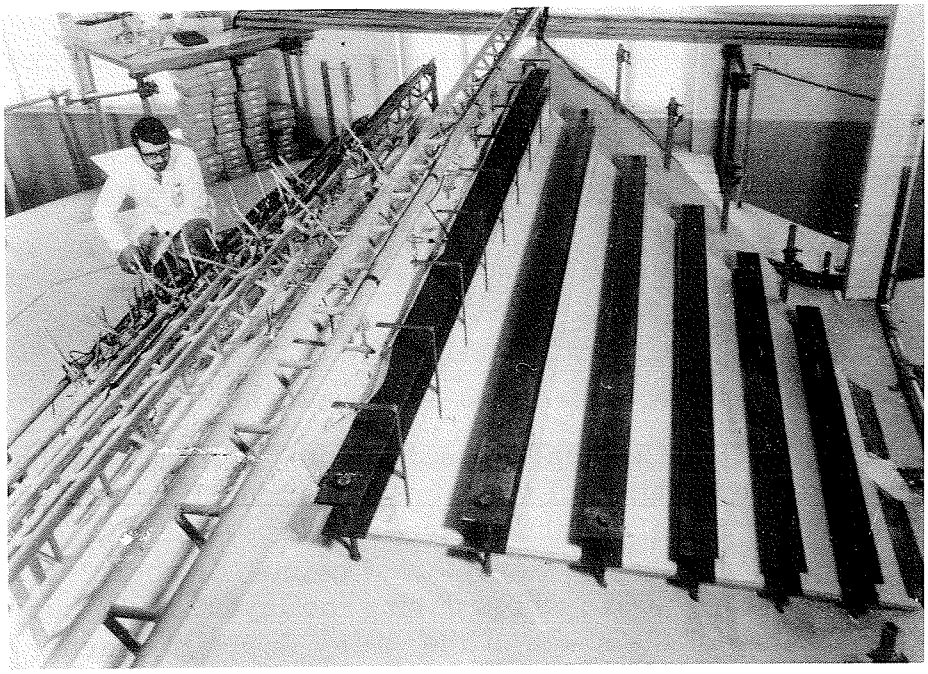

3.3 Testing results

By way of example, a brief summary of the most interesting results obtained during the tests is presented. These results clearly show the influence of the geometric characteristics of the dam on the settlement behaviour of the embankments.

Fig. 12 shows the vertical settlements for dead load effect measured in the central cross section on four different levels and relative to the models indicated. The same settlements are indicated in fig. 13 by means of equal-value curves. It can be easily observed that the vertical settlements appreciably decrease with the increase of the angle of inclination of the lateral abutments. The influence of the inclination of the abutment on the settlement behaviour is considerably greater in

FIG. 12

Vertical settlements for dead-load effect.

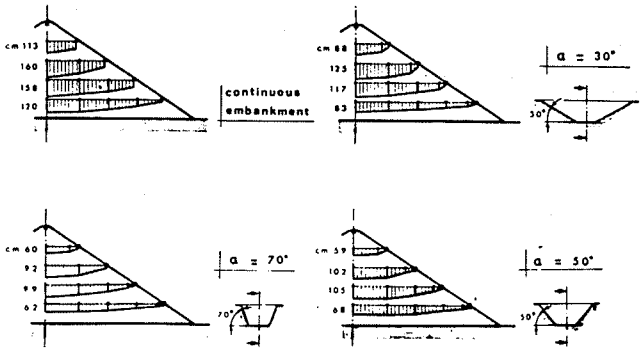

FIG. 13

Equal-value curves of vertical settlement due to dead-load effect.

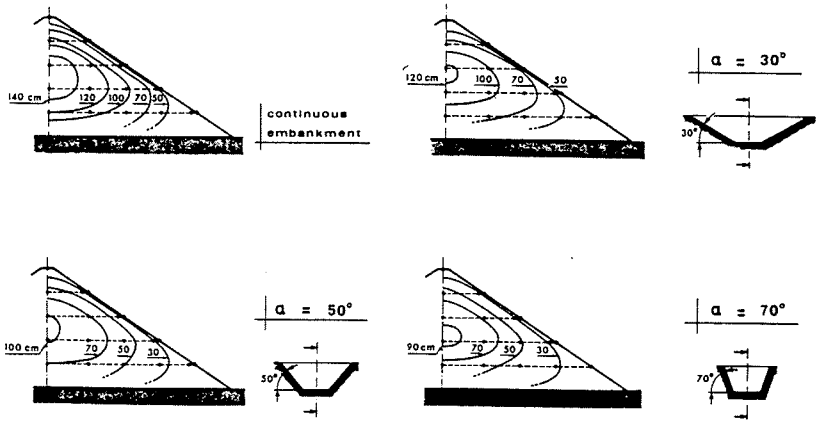

the lateral cross sections of the embankments.

Settlement measurements during the construction of the dam, for the evaluation of the increasing consolidation of the material, are extremely useful for the designer. Fig. 14 and fig. 15 show the settlements measured at two internal points A and B and relative to layers 20 cm and 40 cm thick during the layout of the surrounding layers. The influence of the shape of the valley is clearly seen.

Both vertical and horizontal settlements were measured also during hydrostatic load tests. Fig. 16 shows, as an example, the components of deformation normal to the loaded surface represented by means of equal-value curves and relative to the three models indicated.

The stress-meter cells installed on the foundation facilitated the correct evaluation of the stress distribution at the base of the embankments. Fig. 17 shows the stress distribution curves relative to dead-load effect, while fig. 18 shows the curves relative to the hydrostatic load measured in the central section of the dam. It can be observed that, as the valley narrows, the stresses on the foundation in the main section of the dam rapidly decrease while the component of load normal to the lateral abutments increases. This effect leads to the assumption of behavioural patterns, in the embankment, of the type induced by spatial arches, these latter tending to transfer part of the dead and hydro-

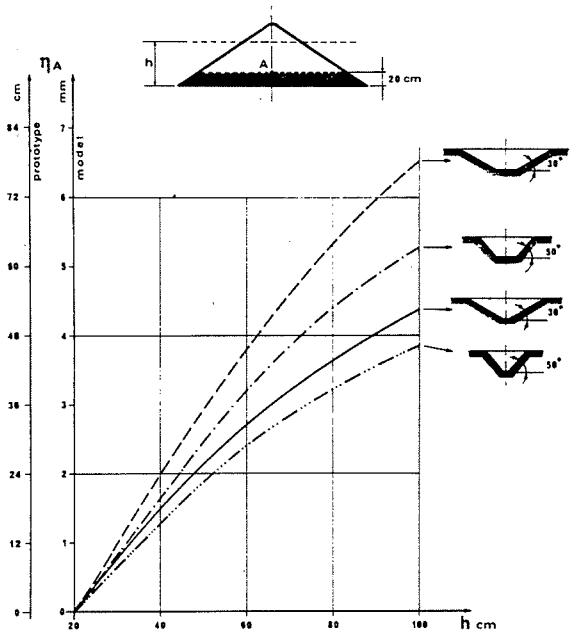

FIG. 14

Vertical settlements of a layer 20 cm thick during the layout of the surrounding layers.

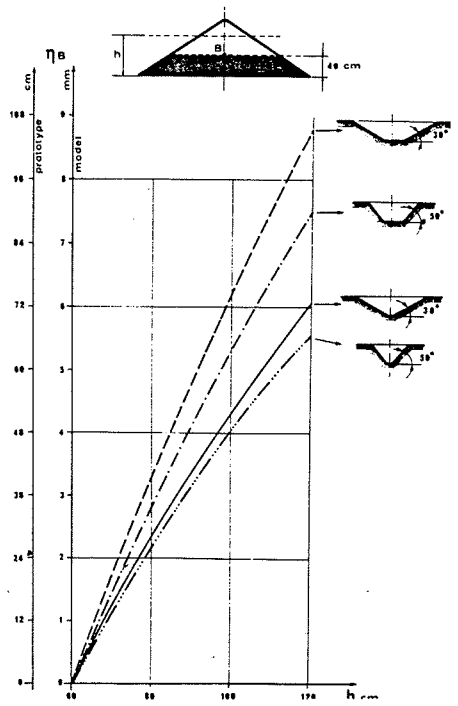

FIG. 15

Vertical settlement of a layer 40 cm thick during the layout of the surrounding layers.

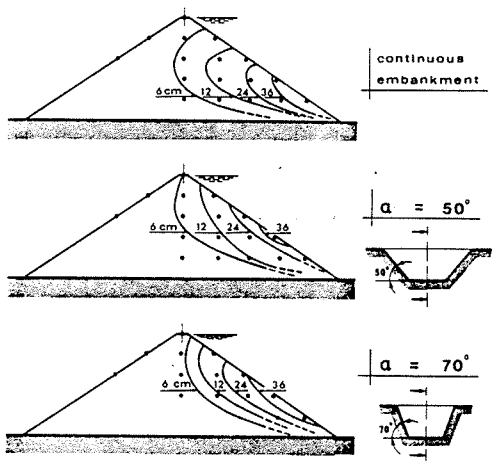

FIG. 16

Equal value settlementd normal to the loading surface hydrostatic load effect.

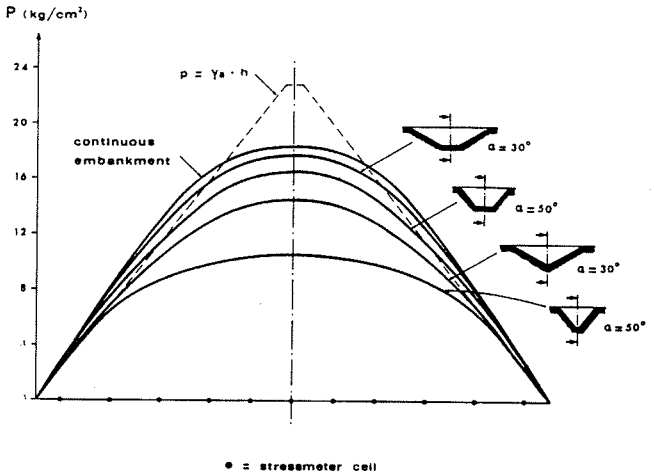

FIG. 17

Pressure distributions on the foundation for dead-load effect.

FIG. 18

Pressure distributions on the foundation for hydrostatic-load effect.

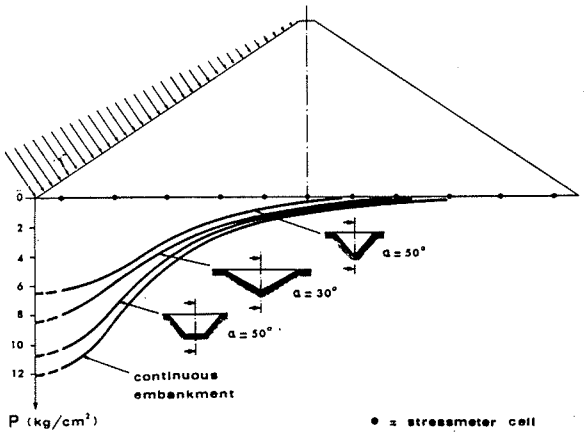

static load onto the lateral abutments.

The results which have been summarized very briefly in this paper merely provide an idea of the large amount of information which can be achieved by a physical model of a rockfill dam. Undoubtely it would be extremely useful for the designer to have a forecast of the behaviour of the dam based not only on the determination of the mechanical characteristics of the prototype granular material, but also on the geometric parameters of the embankment.

4. REFERENCES

1 E. Fumagalli, B. Mosconi: "Esperienze su materiali sciolti di interesse per la progettazione e costruzione delle dighe in rockfill" - IX Congresso AGI, Genova, 1968

2 E. Fumagalli: "Tests on cohesionless materials for rockfill dams" ASCE - Journal of Soil Mechanics and Foundation Division, January 1969

3 E. Fumagalli: "Compression properties of incoherent rock materials for large embankments" - International Conference on Structure, Solid Mechanics and Engineering Design - University of Southampton, Great Britain, April 1969

4 E. Fumagalli, B. Mosconi, P.P. Rossi: "Laboratory tests on materials and static models for rockfill dams" - Proceedings of X Congress on Large Dams, Montreal, Canada, June 1970